

Position control of the Thomson's ring system using fractional operators

Manuel A. Duarte-Mermoud, Norelys Aguila-Camacho and Rafael Castro-Linares

Abstract—The position control of a magnetic levitation system, known as Thomson's ring, is studied in this paper. The design and implementation of three control strategies are presented; the first corresponds to a pole placement control (PPC), the second is a fractional order proportional integral derivative (FOPID) control and the third consists of a sliding mode control (SMC). In all three cases, a fractional order observer is used to estimate the ring speed. A particle swarm optimization (PSO) technique was used in the case of the FOPID control, in order to select the optimal parameters of the controller. Stabilization and tracking experiments are carried out in order to observe the behavior of the controlled system. Also, the effect of external disturbances on the output of the system is addressed.

Index Terms—Magnetic levitation systems, Pole placement control, Fractional order PID, Sliding mode control, Fractional order observers, Thomson's ring.

I. INTRODUCTION

THE materials transport is an important problem in the manufacturing industry. In some cases, the complexity of the transport requirements has led to the need of designing specific transport systems, e.g. minimizing the friction between working surfaces.

The levitation systems (MagLev) have low or non-existent friction side effects, and also have the advantage of operating with low noise levels and the possibility of operating in high vacuum environments. Besides their advantages for the materials transport, the MagLev systems can be applied to another important areas such as microrobotics [1], photolithography [2] and launching systems [3].

In general, a MagLev system can be classified, according to the forces considered on it, as repulsive systems or attractive systems [4]. These systems are also highly nonlinear and unstable in open loop, and for that reason they require control systems to achieve a closed loop stable operation.

Particularly, the MagLev known as "Thomson's ring" was created by Elihu Thomson (1853–1937), and it is composed by an induction coil with a ferromagnetic core and a ring placed in the core (see Figure 1, where a detailed diagram of the system is shown). When an alternate current flows through the coil, a current is induced in the ring. The magnetic field due to this

induced current opposes to the magnetic field induced by the coil, producing a repulsive force between the two elements, and in that way the ring rises above the coil core [5].

As it was mentioned before, the Thomson's ring is an open loop unstable system, and for that reason a control strategy to stabilize the ring in a desired position and to follow a desired trajectory is needed. Some control strategies for this system have been reported in the literature. We can mention the work by García-Antonio et al. [6], where the synchronization of two Thomson's ring modules is addressed, using synchronization techniques proposed in mobile robotics and sliding mode control. More recently, in the work by Ramírez-Neira et al. [7], a linear control of the ring position is addressed, using an active disturbance rejection technique, based on generalized proportional-integral observers. We can also mention the work by Duarte-Mermoud et al. [8], where a Thomson's ring is controlled using a FOPID controller (FOPIDC) and a sliding mode control (SMC). Other works related to magnetic levitation systems can be found in control literature, reporting stabilization via state-PI feedback control [9] and robust feedback control [10], among others.

This paper presents the control of a Thomson's ring, using fractional order control techniques. Particularly, three control schemes are proposed: a pole placement controller (PPC), a FOPIDC and a sliding mode controller (SMC). A fractional order observer is also proposed, in order to estimate the ring speed, which is used in the control techniques. The parameters of the FOPIDC are optimized using particle swarm optimization (PSO), and the behavior of the controllers is shown by numerical simulations, comparing the obtained results. Some robustness experiments are also addressed, where the influence of external disturbances in the system output is considered.

The paper is organized as follows. Section II describes the Thomson's ring system and its dynamical model. Next, some concepts of fractional calculus are presented in Section III. The design of the fractional order observer, the pole placement controller, the FOPID controller and the sliding mode controller are presented and discussed in Section IV, as well as the behavior through numerical simulations. Section V shows the behavior of the three controllers in the presence of external disturbances; and finally, Section VI presents the conclusions of the work.

II. THOMSON'S RING DESCRIPTION

In the Thomson's ring shown in Figure 1, z corresponds to the distance between the ring and the upper point of the coil. The ring moves freely up and down along the core with zero friction. The core is made of a solid ferromagnetic material and

The results reported in this paper have been financed by CONICYT- Chile, under the Basal Financing Program FB0809 "Advanced Mining Technology Center", FONDECYT Project 1150488, "Fractional Error Models in Adaptive Control and Applications"; and FONDECYT 3150007, "Postdoctoral Program 2015".

M. A. Duarte-Mermoud and N. Aguila-Camacho are with the Department of Electrical Engineering and the Advanced Mining Technology Center, University of Chile, Chile (e-mail: mduartem@ing.uchile.cl, naguila@ing.uchile.cl).

R. Castro-Linares is with the Department of Electrical Engineering, Mechatronics Section, CINVESTAV, Mexico (e-mail: rcastro@cinvestav.mx).

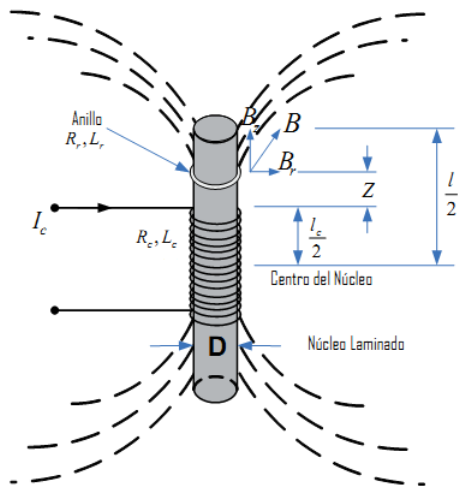


Fig. 1. Thomson's ring diagram.

the ring is made of a non-magnetic conductor (e.g. aluminum or copper).

A sinusoidal input voltage V_c produces an input current I_c circulating in the coil. As a result, a levitation force is generated, acting on the ring and opposed to the effect of gravity. It can be shown ([5] and [11]) that the dynamic of the ring motion is described by the following second order differential equation

$$\ddot{z} = -g + K \frac{V_c^2}{m |Z'_c|^2} z \quad (1)$$

where m is the ring mass, g is the gravity acceleration, V_c is the control input to the system and Z'_c is the ring impedance given by

$$Z'_c = \sqrt{(R'_c)^2 + (\omega L'_c)^2} \quad (2)$$

where ω is the frequency of the sinusoidal voltage applied to the coil and

$$\begin{aligned} R'_c &= R_c - \frac{M_z^2 \omega^2}{|Z_r|} \cos(\phi_r), \\ L'_c &= L_c^s = L_c + \frac{M_z^2 \omega}{|Z_r|} \sin(\phi_r) \end{aligned} \quad (3)$$

R_c and L_c represent the resistance and the inductance of the coil, respectively. M_z is the mutual induction coefficient of the coil-ring system for a fixed distance $z = Z$, ϕ_r is the offset produced by the ring's impedance given by $\phi_r = \arctan\left(\frac{\omega L_r}{R_r}\right)$, being R_r and L_r the resistance and the inductance of the ring respectively. $Z_r = \sqrt{R_r^2 + (\omega L_r)^2}$ represents the impedance of the ring.

The parameter K in Equation (1) is given by

$$K = \frac{M_z^2 \omega}{2 |Z_r|} \sin(\phi_r) \quad (4)$$

It can be seen that this parameter has a rather complex dependence on the magnetic field, the core and ring electrical

circuits and the ring position with respect to the upper side of the coil. In this work, we will consider that K is determined by the nominal equilibrium conditions and it will be assumed to be a constant. Nevertheless, in a real operation and specially in time varying tracking reference problems, the parameter K shows notorious variations that can't be easily measured.

In this study, the parameters of a real Thomson's ring system will be used, since in a second stage it is expected to apply the proposed control techniques at laboratory level. The values of the real parameters are given in Table I [11].

Choosing the state variables $x_1 = z$, $x_2 = \dot{z}$, the state variable representation of system (1) is given by

$$\dot{x} = \begin{bmatrix} \dot{x}_1 \\ \dot{x}_2 \end{bmatrix} = \begin{bmatrix} x_2 \\ -g + \frac{x_2 K}{m |Z'_c|^2} x_1 \end{bmatrix} u \quad (5)$$

where $x = [x_1 \ x_2]^T$ is the state and $u = V_c^2$ is the input to the system. The output of the system corresponds to the ring position i.e. $y = x_1$. If a constant input $u = \bar{u}$ is considered, the the equilibrium point of system (5) becomes

$$\bar{x} = \begin{bmatrix} \bar{x}_1 \\ \bar{x}_2 \end{bmatrix} = \begin{bmatrix} \frac{K \bar{u}}{m g |Z'_c|^2} \\ 0 \end{bmatrix} \quad (6)$$

III. BASIC CONCEPTS OF FRACTIONAL CALCULUS

The fractional calculus is the field that studies integrals and derivatives of orders that can be real or complex numbers [12].

Until the XIX century, fractional calculus was addressed only by some scientists, but later the theory of the fractional calculus was developed, and some applications were studied too. Among them we can mention the electrical networks, the statistic and probabilities, the control theory of dynamical systems, the electrochemical and corrosion, and the theory of chaos and fractals [12].

In the time domain, the fractional derivative and fractional integral are defined by a convolution operation, and that is the reason why they are specially useful to describe some phenomena involving storage or memory. In the Laplace domain, those operations correspond to the operator s^α , with $\alpha \in \mathbb{R}$ [12].

The fractional calculus has gained considerably popularity during the last years in several fields of applications in science and engineering. Some concepts of the traditional calculus that are used in control strategies have been generalized, and therefore designers have found more general solutions exhibiting a better performance. It should be mentioned that in FOPIDC, besides the proportional, integral and derivative

TABLE I
NOMINAL VALUES OF THE THOMSON'S RING PARAMETERS

Parameter	Value
R_r	$0.20816 \times 10^{-3} \ \Omega$
L_r	$2.07023 \times 10^{-6} \ H$
M_z	$36.2 \times 10^{-6} \ H$
V_c	$53.768 \ V$
m	$1.4482 \times 10^{-3} \ Kg$
R_c	$14.5 \ \Omega$
L_c	$128 \times 10^{-3} \ H$

gains, the order of the integral and the order of the derivative parts are also to be chosen by the designer.

In what follows, some basic definitions of the fractional calculus are presented, which will be used along this work.

Definition 1 ([12]): The Riemann-Liouville fractional integral of a function $f(t)$, defined in a finite interval in \mathbb{R}^+ is given as follows:

$$I_a^\alpha f(t) = \frac{1}{\Gamma(\alpha)} \int_a^t \frac{f(\tau)}{(t-\tau)^{1-\alpha}} d\tau \quad (7)$$

where $t > a$, $\Re(\alpha) > 0$ and $\Gamma(\alpha)$ corresponds to the Gamma function [12].

Regarding the fractional derivative, there exist several definitions in the literature. In this work we use the Caputo fractional derivative, because it contains initial conditions of the function and its integer order derivatives, which can be physically interpreted in the classic way.

Definition 2 ([12]): The Caputo fractional derivative of order $\alpha \in \mathbb{R}^+$ of a function $f(t)$, defined in a finite time in \mathbb{R}^+ , is given as follows

$${}^C D_a^\alpha f(t) = \frac{1}{\Gamma(n-\alpha)} \int_a^t \frac{f^{(n)}(\tau)}{(t-\tau)^{\alpha-n+1}} d\tau \quad (8)$$

where $t > a$ and $n = \min \{k \in \mathbb{N}/k > \alpha\}$, $\alpha > 0$.

IV. CONTROL TECHNIQUES USED IN THE STUDY

This section addresses first the design of a fractional order observer, in order to estimate the speed of the ring. This speed estimate will be used as part of the control techniques. After that, the design of a pole placement controller, FOPID controller and a sliding mode controller is presented. The corresponding behavior for stabilization problems and reference tracking problems are simulated towards the end of this section.

A. Fractional order observer for the ring speed

The first problem that arises when controlling system (5), is the fact that only ring position x_1 can be measured. For that reason, this subsection presents the design of a state observer, to estimate the state variable x_2 (ring speed), to be used later in the design of control techniques.

Since the system parameters and model structure are assumed to be known, it is relatively simple to build an observer. From the non linear model of system (5) with output $y = x_1$, the following fractional order state observer is proposed

$$\begin{aligned} {}^C D^\alpha \hat{x}_1 &= \hat{x}_2 + l_1 (\hat{x}_1 - x_1) \\ {}^C D^\alpha \hat{x}_2 &= -g + \frac{K}{m|Z_c|^2} u + l_2 (\hat{x}_1 - x_1) \\ \hat{y} &= \hat{x}_1 \end{aligned} \quad (9)$$

where $0 < \alpha < 2$ and the parameters l_1, l_2 will be defined later. Defining the state estimation errors as

$$\begin{aligned} e_1 &= \hat{x}_1 - x_1 \\ e_2 &= \hat{x}_2 - x_2 \end{aligned} \quad (10)$$

the equations describing the evolution of the errors (10) can be written as

$$\begin{bmatrix} {}^C D^\alpha \hat{x}_1 - \dot{x}_1 \\ {}^C D^\alpha \hat{x}_2 - \dot{x}_2 \end{bmatrix} = \begin{bmatrix} l_1 & 1 \\ l_2 & 0 \end{bmatrix} \begin{bmatrix} e_1 \\ e_2 \end{bmatrix} \quad (11)$$

Equation (11) does not have a known structure, since a fractional order observer has been proposed for an integer order system. On the other hand, there is no analytical proof reported in literature for the stability and convergence of the estimator (9). However, through simulation studies it has been observed that if the parameters l_1 and l_2 are selected such that the matrix

$$\begin{bmatrix} l_1 & 1 \\ l_2 & 0 \end{bmatrix} \quad (12)$$

has real negatives eigenvalues, then the estimation errors (10) converge to zero as t tends to infinity. The roots of the characteristic equation of matrix (12) are given by

$$r_{1,2} = \frac{l_1 \pm \sqrt{l_1^2 + 4l_2}}{2} \quad (13)$$

In order to have real negative eigenvalues, it must be guaranteed that $l_1^2 + 4l_2 \geq 0$, $l_1 < 0$ and $\sqrt{l_1^2 + 4l_2} < |l_1|$. In this study the following values were selected $l_1 = -40$, $l_2 = -400$, corresponding to eigenvalues of matrix (12) located at -20 .

B. Design of pole placement controller (PPC)

The first solution presented for this problem, is the possibility to cancel the system nonlinearities and, at the same time, placing the controlled systems poles at a desired location.

The possibility to cancel the nonlinearities is considered due to the fact that the system parameters are assumed to be known and time invariant, at least from a design point of view. In order to implement this solution, we will assume that the state variable x_2 is accessible, since the fractional order observer designed in Section IV-A will be used in the implementation.

In that way, a control signal is proposed for the system (5) in the form

$$u = \frac{x_1}{K} [g - c_1 x_1 - c_2 x_2 + c_3 v], \quad (14)$$

where $c_1, c_2, c_3 \in \mathbb{R}$ are design parameters and v corresponds to a new input, which in this case will be the desired value for the ring position. The representation of the closed loop resulting systems turns out to be

$$\begin{bmatrix} \dot{x}_1 \\ \dot{x}_2 \end{bmatrix} = \begin{bmatrix} 0 & 1 \\ -c_1 & -c_2 \end{bmatrix} \begin{bmatrix} x_1 \\ x_2 \end{bmatrix} + \begin{bmatrix} 0 \\ c_3 \end{bmatrix} v \quad (15)$$

$$y = [1 \quad 0] \begin{bmatrix} x_1 \\ x_2 \end{bmatrix},$$

with a transfer function given by

$$G(s) = \frac{c_3}{s^2 + c_2 s + c_1}. \quad (16)$$

As can be seen from expression (16), the selection of c_1, c_2 must guarantee that the polynomial $s^2 + c_2 s + c_1$ has roots with negative real parts, in order to assure the closed loop stability. In the same way, choosing $c_3 = c_1$, the ring can be stabilized

at the desired value, since the resulting high frequency gain in (16) would be unitary.

There is no need to use an optimization procedure here to find the controller design parameters, since the only thing we must do is moving the poles away from the origin, in order to achieve a rapid response, and checking that the control effort and the transient response do not result deteriorated. Using this procedure, the design parameters are selected in this work as $c_1 = c_3 = 50$, $c_2 = 15$, which results in the closed loop system having their poles at $r_1 = -5$ and $r_2 = -10$. The variable x_2 used corresponds to \hat{x}_2 , which is taken from the fractional order observer (9).

C. Fractional order proportional, integral and derivative controller (FOPIDC)

The proportional integral and derivative controller (PID) is one of the most used in process control, due to its simplicity. With the introduction of the fractional operators in the control field, the FOPIDC arises. It can be mentioned as one of many examples of FOPIDC, the work by Zamani et al. [13].

The second control strategy for the Thomson's ring is a FOPIDC. The FOPIDC input is the control error, corresponding to $e(t) = r(t) - x_1(t)$, where $r(t)$ is the desired reference for the ring position, and the control signal $u(t)$ is given by

$$u(t) = k_P e(t) + k_I I^\gamma e(t) + k_D {}^C D^\beta e(t) \quad (17)$$

Controller parameters k_P, k_I, k_D , the integration order γ and the derivative order β were obtained through an optimization procedure using particle swarm optimization (PSO) [14]. The objective function to minimize in this case was chosen based on the step response and defined as

$$J = M_p + E_{ss} + t_r + t_s + \int_0^T |r(t) - x_1(t)| dt \quad (18)$$

where M_p corresponds to the overshoot, E_{ss} is the steady state error, t_r is the rising time and t_s is the settling time. The parameters computation in the objective function (18) was done by applying a 15 mm step reference to the control scheme, in a time window of 100 seconds. The integration and derivative orders were selected in the interval (0, 2). The integral term in (18) corresponds to the integral of the absolute value of the control error (IAE), with $T = 100$ seconds.

According to our previous experience using PSO techniques in similar problems, the most relevant parameters used for the PSO algorithm were chosen as

- Swarm size: 100
- Number of iterations: 300
- Initial inertia weight: 0.9
- Final inertia weight: 0.4

As a result of this optimization process, the following controller parameters were obtained:

$$\begin{aligned} k_P &= 7.6690 \times 10^4 & k_I &= 12.013 \times 10^4 \\ k_D &= 7.801 \times 10^4 & & \\ \gamma &= 1 & \beta &= 0.97 \end{aligned} \quad (19)$$

As can be seen, the optimization process gave as the best result a controller with an integer integral part and a fractional

derivative component, but pretty close to 1 (almost a standard PID controller). Thus, the fractional derivative of the error is needed to implement the control scheme. To do this, one option could be to derive directly the error, but the negative influence of the derivation process in the presence of noises it is well known. To avoid that, the fractional derivative was implemented using the output of the fractional order observer designed in Section IV-A. According to the definition of the control error, $\dot{e}(t) = \dot{r}(t) - \dot{x}_1(t)$. Since $\dot{x}_1(t) = x_2(t)$, then the first derivative of the error can be constructed using the first derivative of the reference signal and the signal x_2 , which is obtained from the state observer (\hat{x}_2).

D. Sliding mode controller (SMC)

The third control technique implemented for the Thomson's ring was a SMC, since this is a control technique specially developed for non linear systems. To design the controller, the following change of variable is considered

$$\begin{aligned} e_1 &= x_1 - x_{1d} \\ e_2 &= x_2 - x_{2d} \end{aligned} \quad (20)$$

where x_{1d}, x_{2d} correspond to the desired values for the position and the speed of the ring, respectively. The system can be now described as

$$\begin{aligned} \dot{e}_1 &= e_2 \\ \dot{e}_2 &= -g + \frac{K}{m|Z_c|^2} \frac{u}{e_1 + x_{1d}} - \dot{x}_{2d} \\ y_e &= e_1 \end{aligned} \quad (21)$$

To design a sliding mode control to stabilize system (21), we first choose a function $f(e_1)$ such that the system defined as

$$e_2 = f(e_1) \quad (22)$$

satisfies $\lim_{t \rightarrow \infty} e_1 = 0$. To do this, let us consider the following Lyapunov function candidate

$$V = \frac{1}{2} e_1^2 \quad (23)$$

The first derivative of V along the system (21) turns out to be

$$\dot{V} = e_1 \dot{e}_1 = e_1 e_2 \quad (24)$$

Then if we choose $e_2 = f(e_1) = -k_1 e_1$ with $k > 0$, the first derivative of the Lyapunov function becomes

$$\dot{V} = -k_1 e_1^2 \quad (25)$$

which is negative definite. Therefore it can be concluded that $\lim_{t \rightarrow \infty} e_1 = 0$.

We will now design the sliding surface, in such a way that the convergence of the system to the sliding surface can be guaranteed in a finite time. To this end, let us propose the following sliding surface

$$s = e_2 + k_1 e_1 \quad (26)$$

Therefore

$$\dot{s} = \dot{e}_2 + k_1 \dot{e}_1 \quad (27)$$

Using (21) in (27) we obtain

$$\dot{s} = -g + \frac{K}{m|Z_c|^2} \frac{u}{e_1 + x_{1d}} - \dot{x}_{2d} + k_1 e_2 \quad (28)$$

To select the control signal u such that $\lim_{t \rightarrow \infty} s = 0$, we choose the following Lyapunov function candidate

$$V = \frac{1}{2} s^2 \quad (29)$$

Taking its first derivative along (28) results

$$\dot{V} = s\dot{s} = s \left[-g + \frac{K}{m|Z_c|^2} \frac{u}{e_1 + x_{1d}} - \dot{x}_{2d} + k_1 e_2 \right] \quad (30)$$

Then, if we choose the control signal as

$$u = \frac{(e_1 + x_{1d}) m |Z_c|^2}{K} [g - k_1 e_2 + \dot{x}_{2d} - B \operatorname{sgn}(s)] \quad (31)$$

we get

$$\dot{V} = -B|s| \quad (32)$$

where $B > 0$ is a design parameter to handle the convergence speed.

As can be seen, \dot{V} is negative definite and then it follows that $\lim_{t \rightarrow \infty} s = 0$.

With the control signal defined in (31), the control scheme was implemented. Since e_2 is needed to build the control signal, the fractional observer designed in Section IV-A was used to supply e_2 , as explained in Section IV-C for the FOPIDC.

As in the case of the PPC, no optimization procedure was used here to find the controller design parameters. The selection was made by using our experience in tuning this type of controller, as in the case of the pole placement controller. The design parameters then were selected as $k_1 = B = 25$, in order to obtain a good convergence speed of the errors to zero. The hyperbolic sine function was used instead of the sign function, to avoid chattering effects in the control signal commonly found in this kind of controller [15].

E. Numerical simulations

To verify the behavior of the proposed control schemes, a first experiment was performed, where the control goal is to stabilize the ring in a desired fixed position.

Figure 2 shows the behavior of the PPC, Figure 3 shows the behavior of the FOPIDC and Figure 4 shows the behavior of the SMC, when a 15 mm step reference is applied. The results of several experiments were plotted, for different values of the order α for the fractional observer.

As can be seen from Figures 2, 3 and 4, the stabilization is achieved in the three cases, no matter the order of the fractional observer. In the case of the FOPIDC, all the responses are very similar. It is important to point out that for the FOPIDC, only fractional observers with orders $\alpha \leq 1$ were used, since using orders $\alpha > 1$ lead to a very oscillating transient behavior in the control signal.

Looking at Figure 3 we can note that the response for the FOPIDC is not so fast as in the case of the PPC and the SMC. The step response of the FOPIDC, obtained with the resulting parameters of the optimization procedure, has a settling time

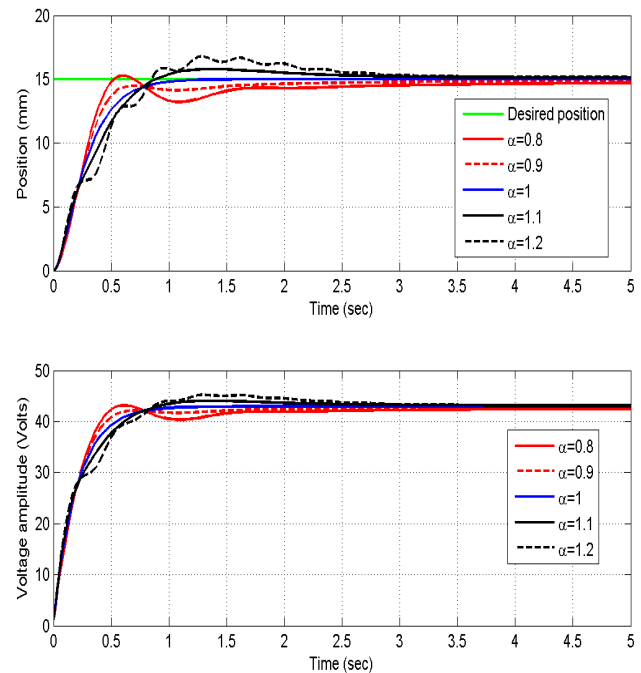


Fig. 2. Behavior of the controlled system using PPC.

equivalent to a system with poles around -2 . Compared to the PPC, which has poles in -5 and -10 , of course the response is slower in the case of the FOPIDC. In the case of the SMC, the response is even more fast than in the case of the PPC, as a result of the chosen design parameters.

It is important to note that the transient response has almost none oscillations in the case of the FOPIDC, no matter the

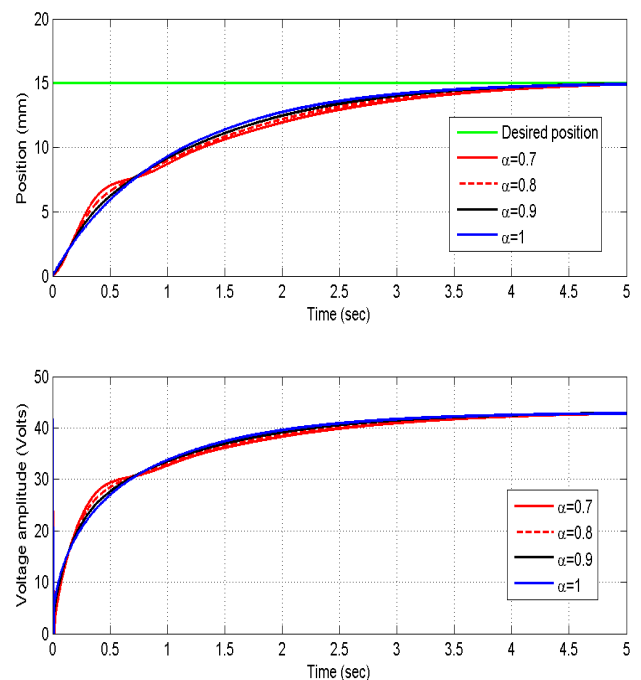


Fig. 3. Behavior of the controlled system using FOPIDC.

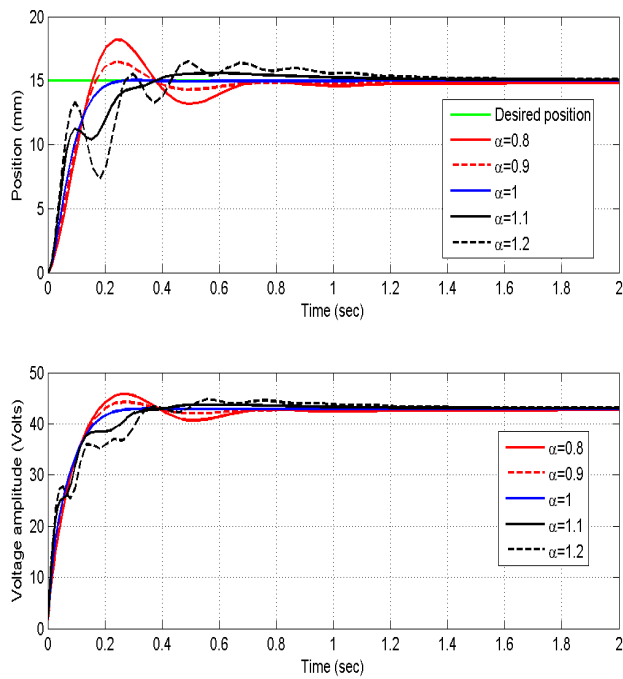


Fig. 4. Behavior of the controlled system using SMC.

fractional order selected for the observer. However, in the case of the SMC and the PPC, the transient response is different depending on the fractional order used in the observer. This difference is more notorious in the case of the SMC than in the case of the PPC.

A second experiment was carried out, where the control goal was tracking a sinusoidal reference signal centered in 15 mm, with amplitude 5 mm and frequency $\pi/6$ rad/s.

Figure 5 shows the behavior of the system using the PPC, and in this case the control error has been plotted instead of the system output.

As can be seen from Figure 5, even though the error remains bounded, it has a considerable magnitude for the PPC. This is due to the fact that the design was made locating the closed loop poles in $r_1 = -5, r_2 = -10$, and the resulting response is not that fast. If a different selection of parameters c_1, c_2, c_3 is made, resulting in closed loop poles farther from the origin, a better tracking will be expected. In order to do that, different values for the design parameters were selected, with the following values; $c_1 = c_3 = 1500$ and $c_2 = 80$. This selection gives closed loop poles in $r_1 = -30, r_2 = -50$, and the response is expected to be faster than in the previous case. Figure 6 shows the behavior of the control error with this new set of design parameter. As expected, a better tracking of the sinusoidal reference signal is achieved in this case. Although there is still an error its magnitude is rather small. This second set of parameters, however, results in a more oscillatory transient response and a higher control effort, so there is a trade off between those aspects.

Figure 7 shows the behavior of the system using FOPIDC, and in this case the control error has been plotted instead of the system output.

As can be seen from Figure 7, the error has a considerable magnitude for the FOPIDC, even when it remains bounded, as it was in the PPC case. In the case of FOPIDC, this is due to the fact that the parameter optimization process was carried out for a step reference. If a new parameter optimization procedure is carried out but using now a sinusoidal reference signal, then different parameters will be found for the FOPIDC. This was done using a different objective function, since most of the parameters in (18) has no meaning if the reference is different from a step. In this new case, the objective function (33) was used, and the resulting parameters are shown in (34).

$$J = \int_0^T t |r(t) - x_1(t)| dt. \quad (33)$$

$$\begin{aligned} k_P &= 1.7754 \times 10^6 & k_I &= 0, 1352 \times 10^6 \\ k_D &= 0, 2213 \times 10^6 & & \\ \gamma &= 1 & \beta &= 0.97 \end{aligned} \quad (34)$$

With this new set of parameters, a better tracking of the sinusoidal reference signal was achieved, as can be seen from Figure 8. Although there is still an error its magnitude is small. This second set of parameters (34) also offers good results in the case of a step reference, but the control effort is higher than that obtained for the previous set of parameters. This is the same that occurred in the previous case with the pole placement controller, where there is a trade off between the convergence speed and the control effort.

Figure 9 shows the evolution of the position error when the reference signal is sinusoidal, using SMC. As can be seen from Figure 9, the error remains bounded, but it does not converge to zero neither, as was in the case of the FOPIDC and the PPC.

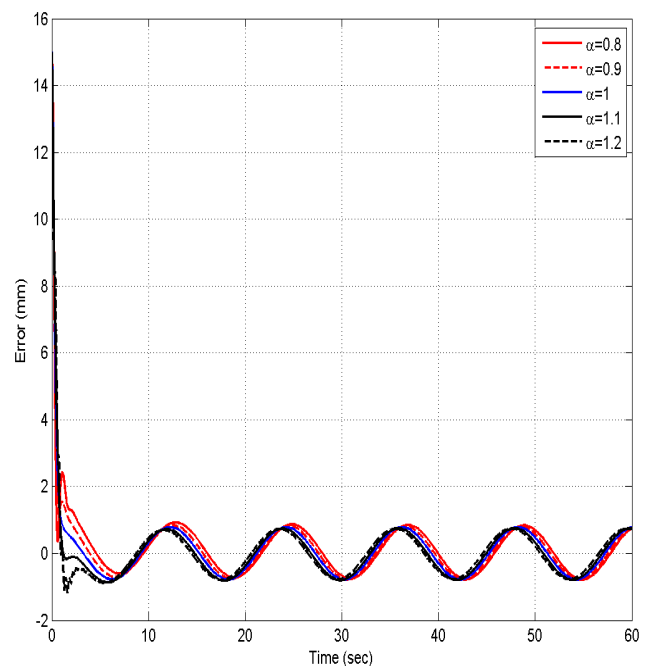


Fig. 5. Evolution of the position error using PPC, when a sinusoidal reference signal is applied.

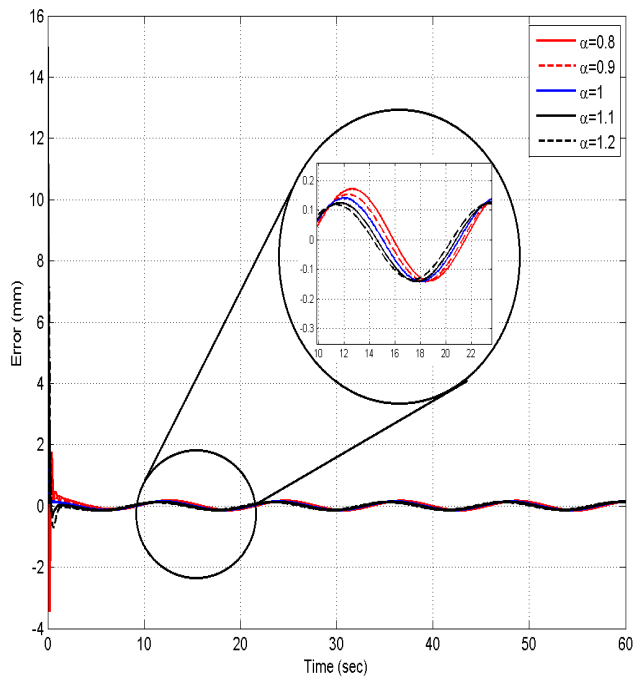


Fig. 6. Evolution of the position error using PPC, when a sinusoidal reference signal is applied and design parameter are selected as $c_1 = c_3 = 1500, c_2 = 80$.

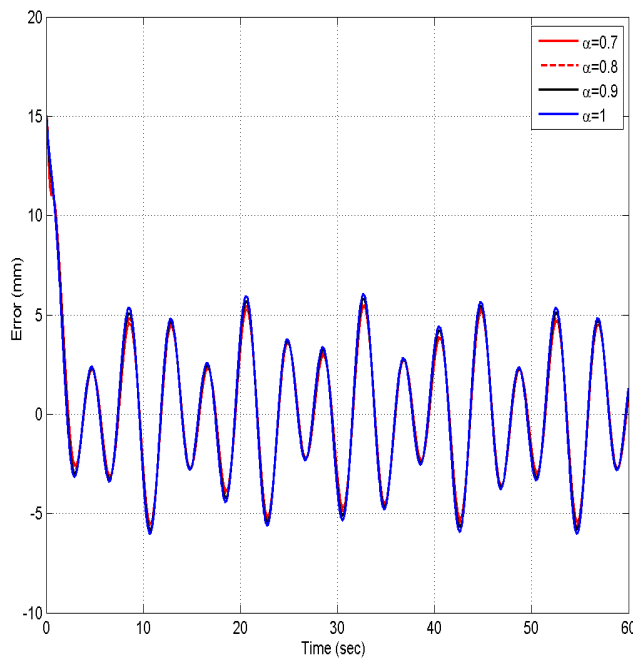


Fig. 7. Evolution of the position error using FOPIDC, when a sinusoidal reference signal is applied.

However, we should mention that in this case the magnitudes of the error are lower than for the case of the FOPIDC, and also with no modifications in the design of the control scheme.

All the results presented in this numerical examples motivates the use of optimization procedures, in order to select

new sets of design parameters for the PPC and the SMC. Doing this, we expect to find the middle point between the convergence speed of the error and the control effort, which is part of the future work.

V. BEHAVIOR OF THE CONTROLLERS IN THE PRESENCE OF EXTERNAL DISTURBANCES

As it is seen from previous experiments, the three control strategies can achieve a satisfactory performance in stabilization problems. In the case of tracking sinusoidal references, there is always a steady state error, although the magnitudes of this error can be decreased if some design parameters are suitably chosen. This behavior was observed for every order α used in the fractional observer.

However, some robustness experiments under disturbances were carried out, to test the behavior of the controllers for different values of order α used in the fractional observer. In one of this experiments, once the system is stabilized in 15 mm, a sinusoidal disturbance is applied to the system output, with amplitude 1 mm and frequency $\pi/2$, specifically at the time instant $t = 60$ seconds. In the case of the FOPIDC the parameter values in (19) were chosen, in the case of the PPC the design parameter $c_1 = c_3 = 1500, c_2 = 80$ were used, and in the case of the SMC the design parameters were $k_1 = B = 25$.

In order to evaluate the behavior of the controlled systems under this external disturbance, the integral of the squared error is plotted in Figure 10, for the three control strategies and for different order α used in the fractional observer.

As can be observed from Figure 10, in the case of using FOPIDC the ISE is pretty similar for every order α used for the fractional observer. However, in the case of the PPC and

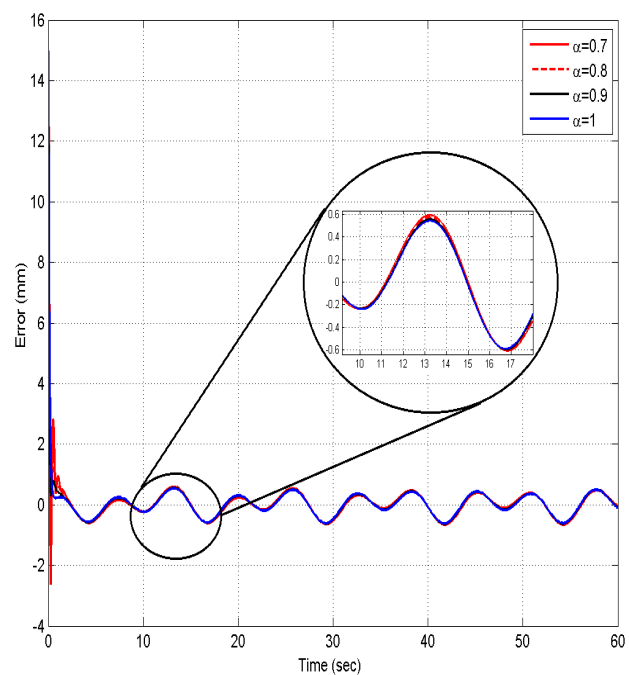


Fig. 8. Behavior of the controlled system using FOPIDC, when a sinusoidal reference signal is applied.

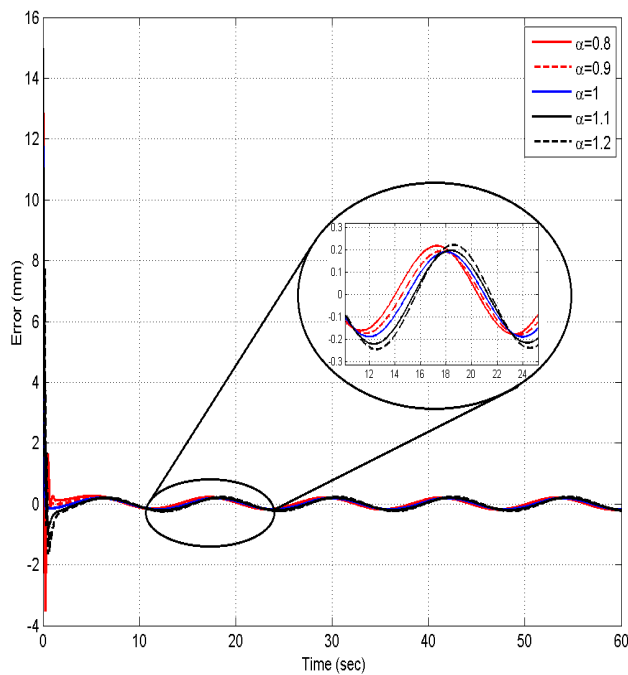


Fig. 9. Evolution of the position error using SMC, when a sinusoidal reference signal is applied.

in the case of the SMC, the lower ISE is achieved with the fractional order $\alpha = 1.1$, that is to say, the controlled system is more robust in the presence of this external disturbance when the observer is of fractional order.

From this simple analysis, it can be concluded that the introduction of the fractional operators in the control schemes can effectively make the system more robust under external disturbances, although the choice of this fractional order not only depends on the system under control but also on the specific control technique used.

VI. CONCLUSIONS

In this work we analyzed the position control in a Thomson's ring magnetic levitation system. In order to achieve this goal, three control strategies were designed, implemented and evaluated. The first one corresponds to a PPC, the second is a FOPIDC and the third one corresponds to a SMC.

In all three cases, a fractional order observer was used to estimate the speed of the ring. The parameters of the FOPIDC were obtained through an optimization problem using PSO, together with an objective function depending on the problem addressed (stabilization or tracking a sinusoidal reference). The three control strategies resulted in a good performance in stabilization problems, and for the case of tracking a sinusoidal reference, a steady state error was obtained. The magnitude of this error can be diminished by handling some design parameters of the controllers. The use of a fractional order in the observer lead to a more robust controlled system, when a sinusoidal external disturbance was applied to the system output.

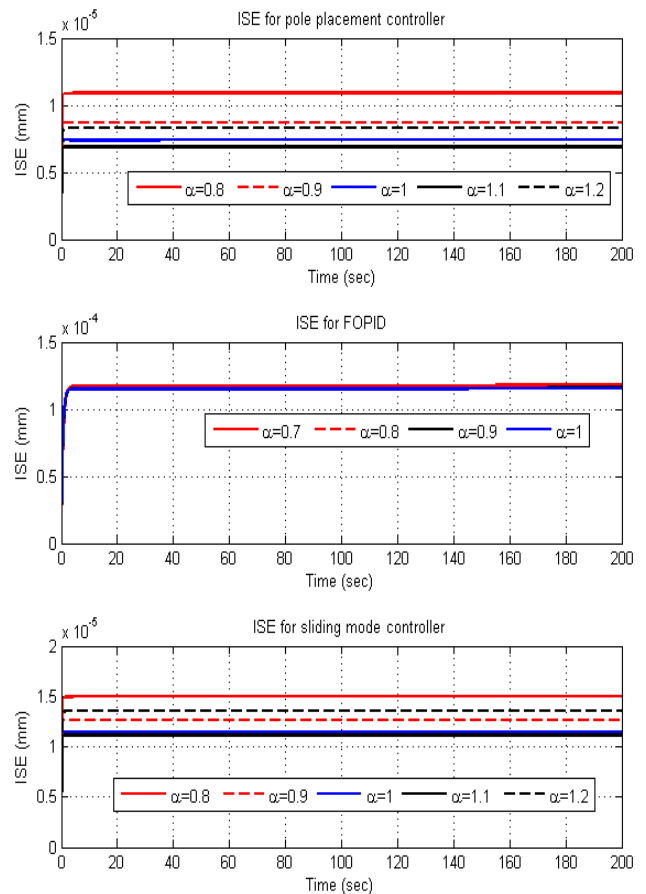


Fig. 10. Integral of the squared error when a sinusoidal external disturbance is applied to the system output, for the three controllers.

All the obtained results motivate the implementation of these control techniques in the real MagLev system, which will be our next step.

ACKNOWLEDGMENTS

This work has been supported by CONICYT- Chile, under the grants FB009 "Centro de Tecnología para la Minería" and FONDECYT 1150488 "Fractional Error Models in Adaptive Control and Applications".

REFERENCES

- [1] Y. Nomura, M. B. Khamesee, N. Kato and T. Nakamura, *Design and control of microrobotic system using magnetic levitation*, IEEE/ASME Transactions on Mechatronics, 7:1-4, 2002
- [2] W. J. Kim and D. L. Trumper, *High-precision magnetic levitation stage for photolithography*, Precision Engineering, 22:66-77, 1998.
- [3] W. A. Jacobs, *Magnetic launch assist-nasa vision for the future*, IEEE Transactions on Magnetics, 37:55-57, 2001.
- [4] I.Y.A. Wang, S.H. Li and I. Buch-Vishniac, *A magnetic levitation transport path*, IEEE Transactions on Semiconductor Manufacturing, 4:145-154, 1991.
- [5] N. Barry and R. Case, *Elihu Thomson's jumping ring in a levitated closed-loop control experiment*, IEEE Transactions on Education, 42:72-80, 1999.
- [6] J. L. García-Antonio, R. Castro-Linares and M. Velasco-Villa, *Synchronization control of a magnetic levitation system powered by alternating current*, 9th International Conference on Control and Automation, 2011.

- [7] M. Ramírez-Neria, J.L. García-Antonio, H. Sira-Ramírez, M. Velasco-Villa and R. Castro-Linares, *On the linear active disturbance rejection control of Thomson's ring*, 2013 American Control Conference, 2013.
- [8] M.A. Duarte-Mermoud, N. Aguila-Camacho and R. Castro-Linares, *Fractional order control of the Thomson's ring magnetic levitation system*, Advances in Electrical and Computer Engineering. Proceedings of the 6th NAUN International Conference on Circuits, Systems, Control and Signals (CSCS '15), Canary Islands, Spain, 40-48, January 2015.
- [9] W. Wiboonjaroen and S. Sujitjorn, *Stabilization of a magnetic levitation control system via state PI feedback*, International Journal of Mathematical Models and Methods in Applied Sciences, 7:717-727, 20143.
- [10] S.K. Choudhary, *Robust feedback control analysis of magnetic levitation system*, WSEAS Transactions on Systems, 13:285-291, 2014.
- [11] J. L. García-Antonio, *Diseño, construcción y control de una plataforma de levitación magnética basado en corriente alterna*, Master Thesis, Centro de Investigación y de Estudios Avanzados del Instituto Politécnico Nacional de México, 2011.
- [12] A. Kilbas, H. Srivastava and J. Trujillo, *Theory and applications of fractional differential equations*, Elsevier, 2006.
- [13] M. Zamani, M. Karimi-Ghartemani, N. Sadati and M. Parniani, *Design of a fractional order PID controller for an AVR using particle swarm optimization*, Control Engineering Practice, 17:1380-1387, 2009.
- [14] A.E. Olsson, *Particle Swarm Optimization: Theory, Techniques and Applications*, Nova Science Publishers Incorporated, 2011.
- [15] H. K. Khalil, *Nonlinear Systems Third Edition*, Prentice Hall, 2002.



Manuel A. Duarte-Mermoud received his Civil Electrical Engineer title from the University of Chile in 1977 and M.Sc., M.Phil. and Ph.D. degrees, all in Electrical Engineering, from Yale University in 1985, 1986 and 1988 respectively.

Currently he is a Professor at the Electrical Engineering Department of the University of Chile. His main research interests are in robust adaptive control (linear and nonlinear systems, integer and fractional), system identification, signal processing and pattern recognition. He is focused on applica-

tions to mining, energy and wine industry, sensory systems and electrical machines and drives.

Professor Duarte is an IFAC member, and former Treasurer and President of ACCA, the Chilean National Member Organization of IFAC, and former Vice-President of the IEEE-Chile.



Norelys Aguila-Camacho received her Automatic Control Engineer title from the Central University in Cuba in 2003, M.Sc. from the Jose Antonio Echeverria Polytechnic Superior Institute of Cuba in 2010 and Ph.D. in Electrical Engineering from the University of Chile in 2014.

Currently she is a Post Doctoral at the University of Chile. Her main research interests are in fractional adaptive control, nonlinear control and system identification. She is currently focused on applications to grinding circuits in mining industry.



Rafael Castro-Linares received his B.S. degree in Communications and Electronics Engineering from the National Polytechnic Institute, Mexico City, Mexico, the M.Sc. degree in Electrical Engineering from CINVESTAV, Mexico City, Mexico, and the Ph.D. degree also in Electrical Engineering from CINVESTAV, Mexico City, Mexico, in 1981, 1982 and 1987, respectively.

Currently he is a Professor at the Department of Electrical Engineering of CINVESTAV, Mexico City. His research interests are in the theory and practice of nonlinear control.

Professor Castro-Linares is a Senior Member of the IEEE (Institute of Electrical and Electronic Engineers).